First-order character of the displacive structural transition in $BaWO_4$*

Tan Da-Yong(谭大勇), Xiao Wan-Sheng(肖万生)†, Zhou Wei(周 微),
Chen Ming(陈 鸣), Xiong Xiao-Lin(熊小林), and Song Mao-Shuang(宋茂双)

Key Laboratory of Mineralogy and Metallogeny, Guangzhou Institute of Geochemistry, Chinese Academy of Sciences, Guangzhou 510640, *China*

(Received 19 December 2011; revised manuscript received 26 February 2012)

Nearly all displacive transitions have been considered to be continuous or second order, and the rigid unit mode (RUM) provides a natural candidate for the soft mode. However, *in-situ* X-ray diffraction and Raman measurements show clearly the first-order evidences for the scheelite-to-fergusonite displacive transition in $BaWO_4$: a 1.6% volume collapse, coexistence of phases, and hysteresis on release of pressure. Such first-order signatures are found to be the same as the soft modes in $BaWO_4$, which indicates the scheelite-to-fergusonite displacive phase transition hides a deeper physical mechanism. By the refinement of atomic displacement parameters, we further show that the first-order character of this phase transition stems from a coupling of large compression of soft BaO_8 polyhedrons to the small displacive distortion of rigid WO_4 tetrahedrons. Such a coupling will lead to a deeper physical insight in the phase transition of the common scheelite-structured compounds.

Keywords: $BaWO_4$, pressure-induced phase transitions, X-ray diffraction, Raman scattering

PACS: 62.50.–p, 63.70.+h, 61.05.cp, 78.30.–j **DOI:** 10.1088/1674-1056/21/8/086201

1. Introduction

Displacive phase transition is an important type of phase transition in minerals.[1] The transition involves only small motions of atoms to change the symmetry of a crystal structure. There exists no energy barrier between the high- and low-symmetry phases in the free-energy landscape at the transition temperature or pressure. The typical examples are phase transitions observed in quartz and perovskite family.[2−4] On cooling, the hexagonal high-temperature β-phase of quartz at 846 K, rotations of the SiO_4 tetrahedra occur around a axis to form the trigonal low-temperature α-phase. For the phase transition of $SrTiO_3$ at 105 K, a rotational displacement of TiO_6 octahedra around a C_4 axis is responsible. In each a case, SiO_4 tetrahedra or TiO_6 octahedra as the buckles of framework do not distort significantly. With regard to these phase transitions that only involve rotations and displacements of rigid SiO_4 tetrahedra or TiO_6 octahedra, the rigid unit mode (RUM) model provides a physical link between the theory and the chemical bonds and validates the application of the soft-mode model.[5,6] However, we find that another incommensurate phase transition not only takes on rotation or displacement of rigid units but also involves a significant distortion of neighbouring regions. So far, little attention has been paid to the first-order signatures, which are corresponding to the critical distortion. The typical example is scheelite-to-fergusonite phase transition in $BaWO_4$.

Like many other ABO_4-type compounds, $BaWO_4$ crystallizes into a tetragonal scheelite-type structure (space group: $I4_1/a$, No. 88, $Z = 4$) under ambient conditions.[7] The Ba and W sites have an S_4 point symmetry, where the W atoms are coordinated by four O atoms, forming isolated nearly regular WO_4 tetrahedra and the Ba cations are coordinated by eight O atoms, forming BaO_8 polyhedrons.[8] At pressures up to about 7 GPa, $BaWO_4$ modified its tetragonal scheelite-type structure into a monoclinic fergusonite-type structure (space group: $I2/a$, No. 15, $Z = 4$)[9,10] and cut off the negative compression of the lowest Raman modes.[11,12] The detailed description of phase transition showed a continuous change in the axial parameters and volume with pressure,[10] despite the

*Project supported by the National Natural Science Foundation of China (Grant Nos. 11179030 and 90714011) and the Knowledge Innovation Project of the Chinese Academy of Sciences (Grant No. KJCX2-SW-N20).

†Corresponding author. E-mail: wsxiao@gig.ac.cn

fact that early study showed a discontinuous fact.[9] The mechanism of phase transition was evidenced further by the analysis of spontaneous strain and the soft mode theory, and a second-order ferroelastic nature was concluded.[13,14] Recently, the synchrotron angle-dispersive X-ray diffraction (ADXRD) measurements in $BaWO_4$ up to 7.5 GPa and 800 K were carried out.[15] The coexistence of the scheelite and fergusonite structures was found under pressure above 7 GPa at room temperature and high temperature. Although a discontinuity between the a axis of scheelite and the c axis of fergusonite appears at the phase transition, the authors stated that there is no observed discontinuity on the other unit-cell parameters within the accuracy of the experiments, and considered that the fergusonite appears as a direct distortion of the scheelite structure. Thus the phase transition is insistently believed to be a second-order ferroelastic transition. However, we noted the fact that the second-order ferroelastic conclusion reflects only the behaviour of WO_4 tetrahedrons as a rigid-unit displacement. The discontinuity of lattice parameters and the coexisting phases that were observed in the scheelite-to-fergusonite transition of $BaWO_4$,[9,11,15] as the important signatures of first-order transition, have not received much recognition. Therefore, critical experiments are needed to reveal the detailed transition mechanism.

In the present paper, by *in-situ* X-ray diffraction (XRD) and Raman measurements in the neighbourhood of the rapid transition under hydrostatic conditions, we show direct evidences for the first-order character of scheelite-to-fergusonite transition in $BaWO_4$, which is believed to undergo a second-order transition. By the refinement of atomic displacement parameters, we further show that the first-order character of this phase transition stems from a coupling of large compression of soft BaO_8 polyhedrons to the small displacive distortion of rigid WO_4 tetrahedrons. Such a coupling will provide an insight into understanding the scheelite-to-fergusonite transition in other scheelite-structured compounds like the molybdates, germanates, and silicates.

2. Experiment

The sample of $BaWO_4$ was synthesized by a conventional solid-state reaction method. The stoichiometric mixture of $BaCO_3$ and WO_3 with both 99.99% purity was heated at 1473 K for 2 h in a platinum crucible. The X-ray diffraction measurement of the product indicates its scheelite structure under ambient conditions. The high pressure angle-dispersive X-ray diffraction and Raman scattering measurements were carried out by a symmetric Mao–Bell type diamond anvil cell (DAC) with 400-μm culet diamond anvils at room temperature. The T301 stainless steel gasket was pre-indented to an initial thickness of about 50 μm and then drilled to give a 120-μm hole serving as the sample chamber. The $BaWO_4$ fine powder was pressed into a pellet with a thickness of about 15 μm, and a piece of sample about 60 μm in diameter with a ruby chip was loaded into the sample chamber. Methanol-ethanol-water mixture of 16:3:1 ratio was used as pressure medium, which is known to remain liquids below 10.5 GPa.[16,17] The pressure was measured by the shift of the R1 photoluminescence line of ruby.[18]

The synchrotron ADXRD patterns were collected with a classic off-line image plate (IP) at the BL-18C station at the Photon Factory, High Energy Accelerator Research Organization (KEK). The incident X-ray beam was collimated to 40 μm in diameter. The wavelength of the monochromated X-ray beam and the distance between the sample and the IP were 0.6198 Å (1 Å=0.1 nm) and 240.887 mm, respectively, which were calibrated with Ag standard sample by the double-cassette method. Each diffraction pattern was collected for 40 min–50 min at room temperature in this study. One-dimensional (1D) diffraction profiles were generated from IP records using WinPIP software. Indexing, structure solution, and Rietveld refinements of the diffraction data were performed using the GSAS package.[19]

High-pressure Raman spectra were recorded by a Renishaw 2000 micro-Raman spectrometer in the backscattering geometry. An argon ion laser operating at a line of 514.5 nm was used as an exciting source. The focused laser spot is smaller than 2 μm in diameter on the sample surface. A thermoelectrically cooled CCD detector was equipped to collect the scattered light dispersed by a 1800-lines/mm grating. All the measurements were carried out during compression and decompression at room temperature. Reasonably good quality Raman data could be obtained with a collection time of about 120 s at a power level of 20 mW.

3. Results and discussion

The typical ADXRD profiles of $BaWO_4$ at several pressures are shown in Fig. 1. Our results show that the observed diffraction peaks shift smoothly with pressure increasing up to 7.2 GPa. However, at 7.7 GPa, some additional diffraction peaks emerge close to the higher 2θ angle in the scheelite-structured $(101)_s$, $(200)_s$, and $(220)_s$ peaks (as marked with down arrows in Fig. 1; the subscript s represents the scheelite structure here and below). At the same time, the $(004)_s$ and $(204)_s$ diffraction peaks broaden asymmetrically and the intensities of the $(312)_s$ and $(224)_s$ peaks redistribute. The intensity of $(220)_s$ peak also becomes weaker. It should be emphasized that, as pressure increases from 7.2 GPa to 7.7 GPa, the $(004)_s$ line of scheelite structure broadens asymmetrically and shifts a little toward the smaller 2θ angle, which indicates that a new diffraction peak occurs at the smaller 2θ angle near the sheelite-structured $(004)_s$ peak (as shown on the top of Fig. 1). This is more obvious in comparison with the profile at 8.3 GPa, in which the corresponding peak becomes narrow and symmetric, and shifts toward the higher 2θ angle as the pressure increases further. The strong $(220)_s$ diffraction peak vanishes completely at 8.3 GPa, and the XRD pattern at this pressure keeps a similar profile to those at 9.1 GPa and 9.7 GPa. These diffraction evidences suggest that a structure transformation occurs at 7.7 GPa and finish quickly at 8.3 GPa. Although the difference between the initial scheelite structure and the high-pressure phase exists as abovementioned in $BaWO_4$, the XRD patterns of the high-pressure phase still preserve most of the diffraction peaks of the low-pressure scheelite phase. The close relation of phases suggests that there may be a topological relation between the scheelite structure and the high-pressure phase. On release of pressure from 9.7 GPa, the highest experimental pressure in this study, the diffraction signals of the scheelite structure are recovered under ambient conditions.

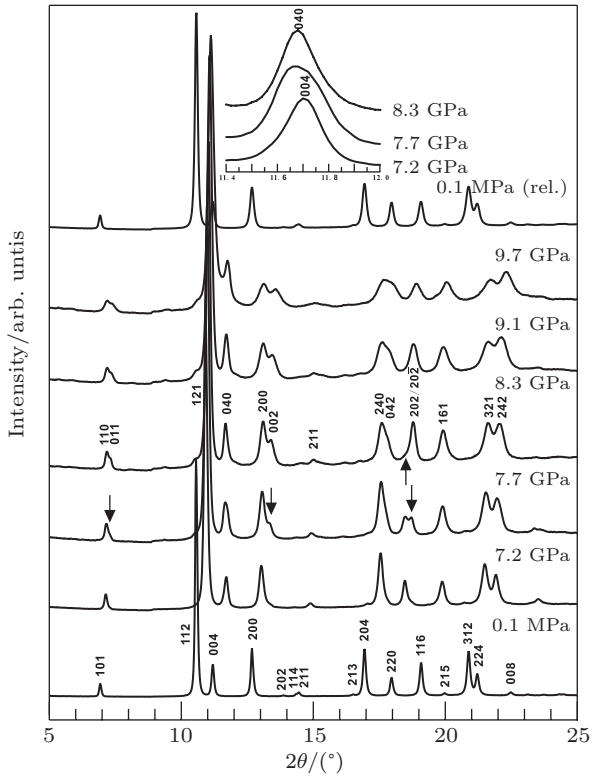

Fig. 1. X-ray powder diffraction patterns of $BaWO_4$ at several pressures. The diffraction patterns at the pressures of 0.1 MPa and 8.3 GPa are indexed as the scheelite and the fergusonite structure respectively. The arrows indicate the appearance or disappearance of the diffraction peak. The inset shows the changes of $(004)_s$ and $(040)_f$ diffraction lines with pressure.

A number of ABX_4-type compounds undergo a temperature or pressure-induced reversible change between the scheelite structure and the fergusonite structure. For example, some rare earth orthoniobates and orthotantalates each with a fergusonite structure at room temperature are converted into the scheelite structures at high temperature.[20−22] $YLiF_4$ undergoes the scheelite-to-fergusonite transition at high pressure.[23] Several orthotungstates and orthomolybdates each with a scheelite structure under ambient conditions, such as $CaWO_4$, $SrWO_4$, $SrMoO_4$, $BaMoO_4$, are also reported to undergo this kind of reversible structural transformation at high pressure.[24−27] Moreover, $BaWO_4$ was also suggested to experience this transition at about 7 GPa.[9,10,28] In the light of the geometrical relationship of the unit cells between the tetragonal scheelite structure ($I4_1/a$) and the monoclinic fergusonite structure ($I2/a$), the fergusonite structure is only a slightly distorted scheelite structure with the cations deviating a little from the special Wyckoff positions and the anions dividing into two kinds of Wyckoff positions accompanied by fractional coordinate displacement, thereby inducing a lower symmetry.[14] This kind of group–subgroup relation indicates a ferroelastic characteristic phase transition. Combining the above analysis with the diffraction features of the pressure-induced phase transition of $BaWO_4$ in this study, it is logical to suggest that the high-pressure phase is responsible for the fergusonite structure. Ri-

etveld refinement of the diffraction patterns was carried out by employing the GSAS programs to index the diffraction lines and extract the structural parameters of both phases. The refinement results for a tetragonal scheelite phase pattern collected at 7.2 GPa, a monoclinic fergusonite phase pattern at 8.3 GPa as well as the two-phase coexisting pattern at 7.7 GPa are shown in Fig. 2. The fitting of the data shows good results for the scheelite and fergusonite structure with residual values $\chi^2 = 0.2680$, $R_{\rm p}(\%) = 3.99$, and $R_{\rm wp}(\%) = 5.23$ at 7.2 GPa, $\chi^2 = 0.3622$, $R_{\rm p}(\%) = 3.06$, and $R_{\rm wp}(\%) = 3.89$ at 7.7 GPa, and $\chi^2 = 0.2606$, $R_{\rm p}(\%) = 3.13$, and $R_{\rm wp}(\%) = 4.23$ at 8.3 GPa.

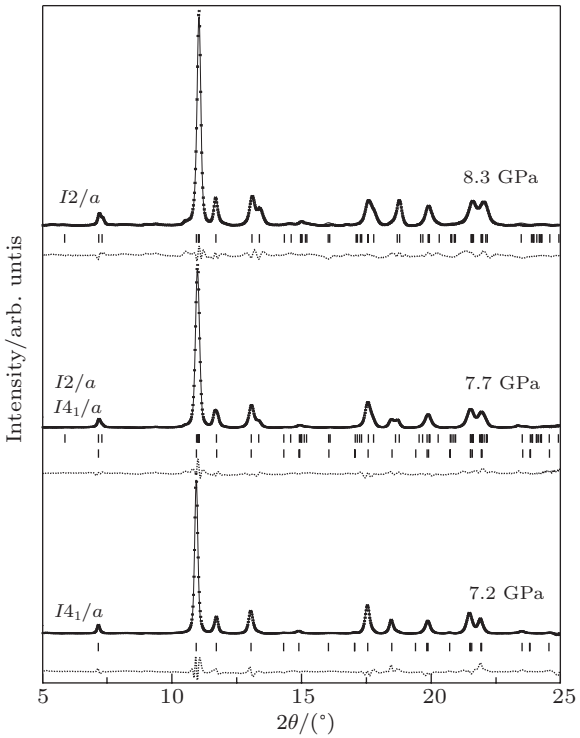

Fig. 2. Rietveld refinement of the $BaWO_4$ ADXRD patterns at the pressures of 7.2, 7.7, and 8.3 GPa. The scheelite ($I4_1/a$), fergusonite ($I2/a$), and two-phase mixed structures are used to fit the patterns. The difference (dotted line) between the observed (crosses) and the fitted pattern (thin line) is shown on the same scale. The vertical bars indicate the calculated positions of the reflections.

Table 1 shows the observed and calculated d-spacings for $BaWO_4$ with the scheelite and the fergusonite structures at pressures of 7.2, 7.7, and 8.3 GPa, respectively. Here we focus on the result at 7.7 GPa since it presents the clear evidences of revealing the first-order ferroelasitc properties of the scheelite-to-fergusonite transition in $BaWO_4$. The co-existence of the $(220)_{\rm s}$ peak and the $(202)_{\rm f}$ peak (the subscript f denotes the fergusonite structure here and below) in the 7.7-GPa pattern indicates that there is a pressure-induced mixed-phase regime of both lower-pressure scheelite phase and high-pressure fergusonite phase, which is an important criterion for the first-order phase transition. Furthermore, the volume change ($\sim 1.6\%$) between both phases and the discontinuities of the $b_{\rm f}$ and $c_{\rm f}$ axes compared with the corresponding $c_{\rm s}$ and $b_{\rm s}$ axes at 7.7 GPa also demonstrate that it is a first-order phase transition. While the subtle difference between the $(040)_{\rm f}$ and $(004)_{\rm s}$ suggests a slight increase in the $b_{\rm f}$ axis compared with the $c_{\rm s}$ axis ($\sim 0.7\%$), and the d-spacing of $(200)_{\rm f}$ is almost the same as that of the $(200)_{\rm s}$, reflecting the nearly equivalent $a_{\rm f}$ axis and $a_{\rm s}$ axis across the phase transition. At the same time, the distinct decrease of the d-spacing of the $(002)_{\rm f}$ to the $(200)_{\rm s}$ [also the $(200)_{\rm f}$], in which they are the topologically associated crystal planes between fergusonite and scheelite structures, indicates that the $c_{\rm f}$ axis shortens markedly ($\sim 2.1\%$) compared with the geometrically related $b_{\rm s}$ axis ($b_{\rm s} = a_{\rm s}$) when phase transition takes place. The abrupt shortening of $c_{\rm f}$ axis leads the $(220)_{\rm s}$ peak to disappear and the $(202)_{\rm f}$ peak to occur at the higher 2θ angle. The remarkable splits of the $(110)_{\rm f}$ and $(011)_{\rm f}$ pairs and the $(240)_{\rm f}$ and $(042)_{\rm f}$ couples also result from the $c_{\rm f}$-axis shortening. In addition, the indistinguishable $(202)_{\rm f}$ and $(20\text{-}2)_{\rm f}$ pairs and some other overlapped peaks in the fergusonite phase suggest that the monoclinic β angle is very close to 90°.

Table 1. Observed and calculated d-spacings for $BaWO_4$ with the scheelite and the fergusonite structures at pressures of 7.2, 7.7, and 8.3 GPa.

	Scheelite					Fergusonite			
	7.2 GPa		7.7 GPa			7.7 GPa		8.3 GPa	
(hkl)	$d_{\rm obs}$/Å	$d_{\rm cal}$/Å	$d_{\rm obs}$/Å	$d_{\rm cal}$/Å	(hkl)	$d_{\rm obs}$/Å	$d_{\rm cal}$/Å	$d_{\rm obs}$/Å	$d_{\rm cal}$/Å
(101)	4.9758	4.9777	4.9600	4.9666	(110)	4.9600	4.9644	4.9469	4.9607
					(011)	4.8852	4.8846	4.8568	4.8739
(112)	3.2532	3.2573	3.2427	3.2493	(121)	3.2386	3.2294	3.2240	3.2295
					(12-1)		3.2278		3.2170
(004)	3.0399	3.0395	3.0292	3.0273	(040)	3.0546	3.0493	3.0455	3.0408

Table 1. (*Continued*).

	Scheelite					Fergusonite			
	7.2 GPa		7.7 GPa			7.7 GPa		8.3 GPa	
(hkl)	d_{obs}/Å	d_{cal}/Å	d_{obs}/Å	d_{cal}/Å	(hkl)	d_{obs}/Å	d_{cal}/Å	d_{obs}/Å	d_{cal}/Å
(200)	2.7303	2.7280	2.7214	2.7229	(200)	2.7214	2.7174	2.7158	2.7166
					(002)	2.6678	2.6654	2.6558	2.6598
(211)	2.3926	2.3923	2.3875	2.3876	(211)	2.3782	2.3753	2.3710	2.3779
(204)	2.0311	2.0302	2.0288	2.0245	(240)	2.0288	2.0287	2.0253	2.0259
					(042)	2.0080	2.0068	1.9976	2.0020
(220)	1.9306	1.9280	1.9285	1.9254	(202)	1.9040	1.9035	1.8990	1.9057
					(20-2)		1.9022		1.8954
(116)	1.7948	1.7939	1.7931	1.7875	(161)	1.7931	1.7932	1.7914	1.7998
					(-161)		1.7929		1.7876
(215)	1.7220	1.7223	1.7215	1.7173	(251)	1.7215	1.7187		
(312)	1.6612	1.6598	1.6581	1.6564	(321)	1.6581	1.6515	1.6517	1.6526
					(-321)		1.6509		1.6476
					(123)	1.6283	1.6280	1.6228	1.6269
					(-123)		1.6274		1.6220
(224)	1.6303	1.6287	1.6256	1.6246	(242)	1.6150	1.6147	1.6166	1.6148
					(-242)		1.6139		1.6085
(008)	1.5202	1.5198	1.5153	1.5136	(080)	1.5299	1.5246		
a/Å	5.4559(3)		5.4458(6)		a/Å	5.4349(13)		5.4332(7)	
c/Å	12.158(1)		12.109(2)		b/Å	12.197(3)		12.163(2)	
					c/Å	5.3308(11)		5.3197(8)	
					β/(°)	89.96(4)		89.69(3)	
V/Å^3	361.91(1)		359.11(2)		V/Å^3	353.38(3)		351.54(2)	

Table 2 shows the structural parameters of $BaWO_4$ with the scheelite structure at 7.2 GPa and the fergusonite structure at 8.3 GPa as obtained through the Rietveld refinements. Due to the topological relation between the two structures, we can compare the corresponding atomic fractional coordinations to understand the atomic displacement across the phase transition, and thus to illustrate the atom moving picture of the phase transition. The corresponding relations of atomic coordination between the two structures are $x_f \to y_s$, $y_f \to z_s$, and $z_f \to x_s$. It is feasible especially for the cations, because the W atoms and the Ba atoms are at the special Wyckoff positions in both structures. In the process of phase transition, the W atoms and the Ba atoms shift only along the scheelite-structured c axis (equivalent to the fergusonite-structured b axis). As for the oxygen atoms, because they occupy the general Wyckoff positions in both structures, their motions appear to be somewhat complicated when phase transition occurs. Here we pay attention only to their shifting along the c_s-axis direction, and we do the same way for the Ba atoms and W atoms. Figure 3 shows the schematic diagram of the scheelite structure along the (010) plane, in which the atomic shifts across the phase transition are labeled with arrows. While the Ba atoms appear as slight displacement ($\Delta z_s = -0.0016$), the W atoms shift about 3 times the magnitude ($\Delta z_s = 0.0046$). As a result, the W atoms and the Ba atoms in the same $(001)_s$ layers move off the special Wyckoff positions in the opposite directions. The oxygen atoms move along with the W atoms as a rigid WO_4 tetrahedron, which is also supported by the minor change of the W–O distance. The W–O distance decreases about 0.2% from 1.7854 Å at 7.2 GPa to an average 1.7826 Å at 8.3 GPa. The trivial difference between the two kinds of W–O distances (1.7819 Å and 1.7832 Å) reflects the quite regular WO_4 tetrahedron in the fergusonite phase, which is also demonstrated by the Raman results as discussed in the following section. In the meantime, the average Ba–O distance decreases about 1.2% from 2.6359 Å to 2.6051 Å. Thus the volume discontinuity results mostly from the volume collapse of the BaO_8 polyhedron as the phase transition occurs. This kind of atomic picture of phase transition provides clear evidence of the first-order ferroelastic character. In particular, when we consider the displacement of the WO_4 tetrahedron as a whole, the ferroelastic characteristic of the phase transition is much clearer. In fact, the atomic moving manner is consistent with the B_g soft mode of the scheelite structure.[14]

Table 2. Structural parameters for the scheelite ($I4_1/a$) phase at 7.2 GPa and the fergusonite ($I2/a$) phase at 8.3 GPa in $BaWO_4$ obtained by the Rietveld analysis.

Structural parameters of scheelite $BaWO_4$ at 7.2 GPa: $I4_1/a$, $Z = 4$, $a = 5.4559(3)$ Å, $c = 12.158(1)$ Å.				
Atom	Site	x	y	z
Ba	$4b$	0	0.25	0.625
W	$4a$	0	0.25	0.125
O	$16f$	0.2307	0.1098	0.0420
Bond lengths/Å				
W–O	1.7854(1)×4	Ba–O	2.6206(2)×4	
		Ba–O	2.6512(1)×4	
Structural parameters of fergusonite $BaWO_4$ at 8.3 GPa: $I2/a$, $Z = 4$, $a = 5.4332(7)$ Å, $b = 12.163(2)$ Å, $c = 5.3197(8)$ Å, $\beta = 89.69(3)°$.				
Atom	Site	x	y	z
Ba	$4e$	0.25	0.6234	0
W	$4e$	0.25	0.1296	0
O1	$8f$	0.8908	0.9553	0.2312
O2	$8f$	0.4814	0.2110	0.8508
Bond lengths/Å				
W–O1	1.7819(2)×2	Ba–O1	2.6078(3)×2	
W–O2	1.7832(2)×2	Ba–O1	2.6078(4)×2	
		Ba–O2	2.6128(3)×2	
		Ba–O2	2.5919(4)×2	

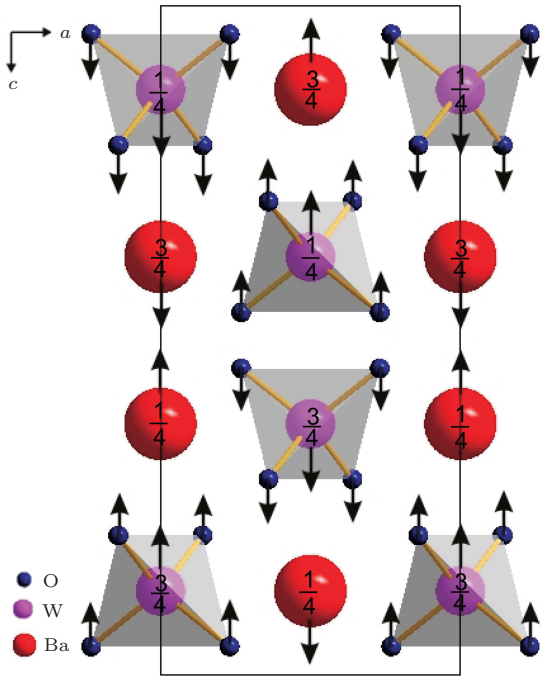

Fig. 3. (colour online) Projection of the scheelite $BaWO_4$ along b axis, the numbers on patterns are y parameters of the Ba and W atoms. The arrows point to the atomic moving directions along the c_s axis while the structure changes from scheelite to fergusonite phase. It illustrates clearly that the WO_4 tetrahedrons displace as a whole in the direction opposite to that of Ba atoms in the same $(001)_s$ layers.

By comparison, the high-pressure XRD research and Rietveld analysis of $BaMoO_4$[26] provide a distinct atomic moving picture while the phase transition from scheelite to fergusonite structure takes place. Therefore it is concluded that all the atoms of alternate layers of the scheelite structure need to shift in opposite directions along the c axis. Comparing the fractional coordinates of Ba atoms and Mo atoms in the fergusonite structure at 7.2 GPa[26] with those of Ba atoms and W atoms in the fergusonite structure in this study and also with those of the special Wychoff positions of the corresponding atoms in the scheelite structure, we could find that the moving directions of Ba atoms and Mo atoms along the scheelite-structured c axis are actually opposite in the same layers, and are the same as that shown by our results, although the magnitudes are smaller than our results.

The first-order ferroelastic mechanism of the scheelite-to-fergusonite phase transition of $BaWO_4$ is also supported by our Raman data. Figure 4 shows the Raman spectra in a range of 100 cm^{-1}–1000 cm^{-1} of $BaWO_4$ at some representative pressures. The Raman spectra of fergusonite $BaWO_4$ each show a phonon gap between 450 cm^{-1}–750 cm^{-1} and an intense and high frequency Raman mode, which are similar to the ones observed in scheelite $BaWO_4$, but are different from the Raman spectra of $BaWO_4$-II phase[29] and the observed results in Ref. [12]. This result not only indicates that the fergusonite phase retains the tetrahedral W–O coordination of the scheelite phase, but also allows us to draw a conclusion that there are no Raman modes belonging to $BaWO_4$-II phase, in the modes observed at high pressure.

In order to analyse the subtle phonon change from scheelite to fergusonite structure, Fig. 5 shows several Raman spectra in a range of 750 cm^{-1}–1000 cm^{-1}, reflecting the stretching vibration modes of WO_4 tetrahedron. Of the Raman modes, the most intense and the highest frequency Raman mode (A_g) is at 947 cm^{-1} at 7.4 GPa, which represents the symmetrical stretching mode of WO_4 tetrahedral units in the scheelite structure.[30] Up to 7.8 GPa, the 947 cm^{-1} peak broadens and drops sharply to 944 cm^{-1}, and a low intensity 903 cm^{-1} band arises. At the same time, several new Raman modes emerge near the E_g (820 cm^{-1}) and B_g (847 cm^{-1}) modes of the scheelite phase. The 7.8-GPa spectrum indicates a coexistence of phases, and the 8.0-GPa spectrum indicates that the phase transition is complete with the scheelite

structural 820 cm^{-1} and 847 cm^{-1} modes disappearing. The changes in Raman spectrum suggest that the WO_4 tetrahedrons modify slightly through the phase transition, and a lower symmetrical phase is formed quickly. Upon decompression from 9.4 GPa, the highest pressure of the Raman experiments, the scheelite phase is recovered completely at 5.6 GPa with a remarkable hysteresis. The Raman results are consistent well with our XRD results.

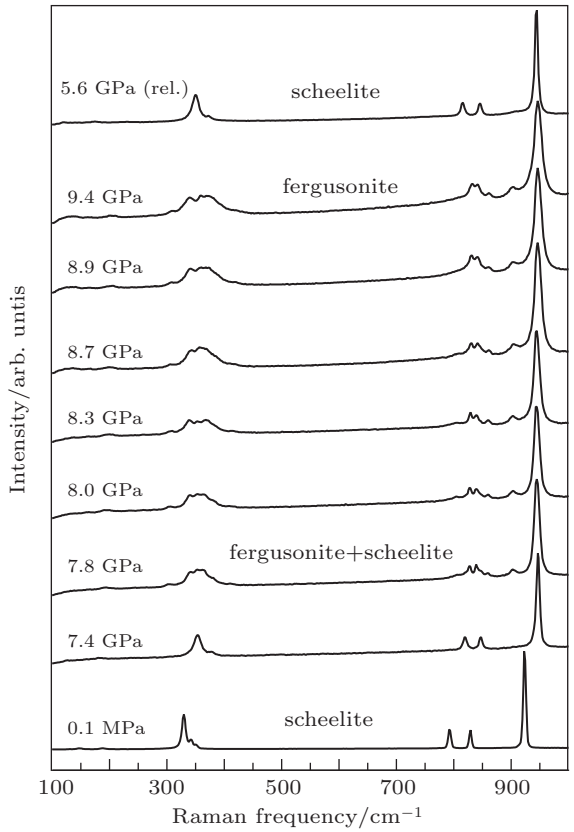

Fig. 4. Raman spectra in a range of 100 cm^{-1}–1000 cm^{-1} of $BaWO_4$ at some representative pressures.

The axial parameters and volume ratio (V/V_0) each as a function of pressure of the scheelite and fergusonite phases of $BaWO_4$ are shown in Fig. 6. We find that two axial parameters of the unit cell change inconsistently across the phase transition, except that the a_s axis and also the corresponding a_f axis decrease smoothly with pressure increasing. The b_s axis shows an obvious reduction ($\sim 2.1\%$) as it transforms to the c_f axis, and the c_f axis decreases as pressure increases further. The c_s axis increases slightly ($\sim 0.7\%$) as it becomes the b_f axis, and the b_f axis begins to decrease as pressure increases further. The changes of the axial parameters result in a 1.6% volume collapse when phase transition occurs. The results are consistent approximately with those of another study in $BaWO_4$[9] and similar to those in $BaMoO_4$.[26] Carefully checking Fig. 2 in previous research of $BaWO_4$[15], we will find a similar trend of lattice parameters varying with pressure to ours, although the authors explained it in another way. Fitting the P–V data of the scheelite phase of $BaWO_4$ by the third-order Birch–Murnaghan equation of state (EOS), gives the bulk modulus (K_0) as 58(1) GPa when its pressure derivative (K_0') is assumed to be 4. It accords generally with $K_0 = 57$ GPa as $K_0' = 3.5$[9] and $K_0 = 52(5)$ GPa as $K_0' = 5(1)$.[10]

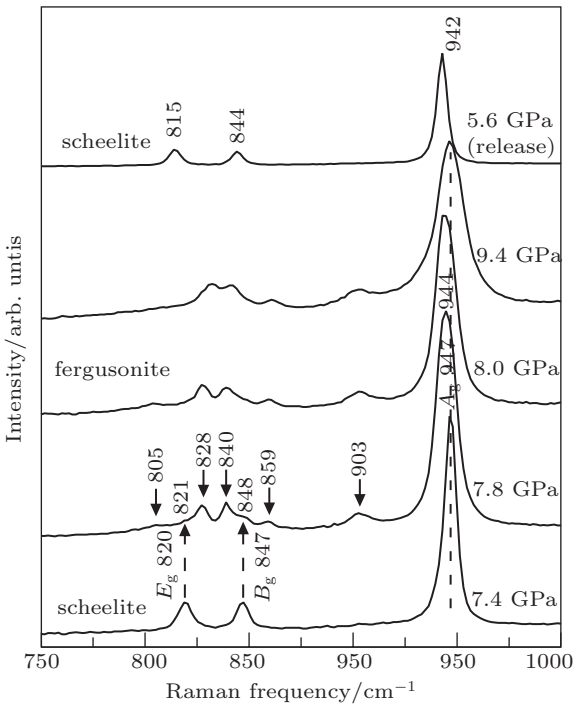

Fig. 5. Several representative Raman spectra of $BaWO_4$ in a range of 750 cm^{-1}–1000 cm^{-1}. The 7.8-GPa spectrum shows the two-phase mixed signatures. The down arrows indicate the new Raman modes. The up arrows indicate the survival Raman modes. The shift of the most intensity Raman mode with pressure increasing is displayed clearly by the dotted line.

In contrast, Errandonea *et al.*[10] reported on completely different evolutions of lattice constant and volume with pressure as scheelite-structured $BaWO_4$ transforms into the fergusonite structrure. Their results show that the a_s axis ($= b_s$ axis) splits continuously to form an increasing a_f axis and decreasing c_f axis with pressure increasing. At the same time, the c_s axis transforms into the b_f axis with no observable discontinuity. Based on the continuous changes of lattice constants and volume with pressure, a second order

nature of the phase transition is concluded. The authors also debated the difference between these results and Panchal *et al.*'s,[9] and considered that due to the restricted XRD measurement performed by Panchal *et al.*, the lower resolution and the smaller access to the reciprocal space would lead to a larger uncertainty in the lattice parameters. Recently, Lacomba-Perales *et al.*[15] pointed out that the different behaviours observed in different experiments could be related to the existence of pressure gradients in the particular experimental set up. As a typical example, the phase transitions of $CuGeO_3$ follow two distinct paths depending on the different pressure media.[31,32] For scheelite-structured $BaWO_4$, Errandonea *et al.*[10] performed the diffraction experiments using silicone oil as pressure medium, but in Panchal *et al.*'s experiment[9] and in the present study is used either 4:1 methanol–ethanol or 16:3:1 methanol–ethanol–water mixture. In fact, silicone oil really exhibits a different hydrostatic behaviour when 4:1 methanol–ethanol or 16:3:1 methanol–ethanol–water mixture is under a pressure at least below 12 GPa.[16,17] Unfortunately, Manjón and Errandonea also reported on a completely different Raman result that scheelite $BaWO_4$ transforms into the $BaWO_4$-II phase at 6.9 GPa, then into the fergusonite structure at 7.5 GPa, finally into the scheelite, $BaWO_4$-II and fergusonite coexist up to 9.0 GPa, although 4:1 methanol–ethanol is used as medium. The single crystal Raman study of $BaWO_4$ is not only inconsistent with their diffraction results,[10] but also dissimilar to those of the previous Raman study[11] and our Raman data. The appearance of $BaWO_4$-II phase and lower phase transition pressure may be caused by the non-hydrostatic surface environment of the single crystal with 30 μm in thickness. In any case, from the view of hydrostatic condition, there may be another scientific cause that a slight difference of hydrostatic circumstance would induce first or second-order competitive phase transitions in $BaWO_4$. Nevertheless, on the basis of our own consistent diffraction and Raman experiments and the work of Jayaraman *et al.*[11] and Panchal *et al.*[9] using methanol–ethanol-water or methanol–ethanol mixture as a pressure medium, we support that the scheelite-to-fergusonite transition in $BaWO_4$ is of the first order.

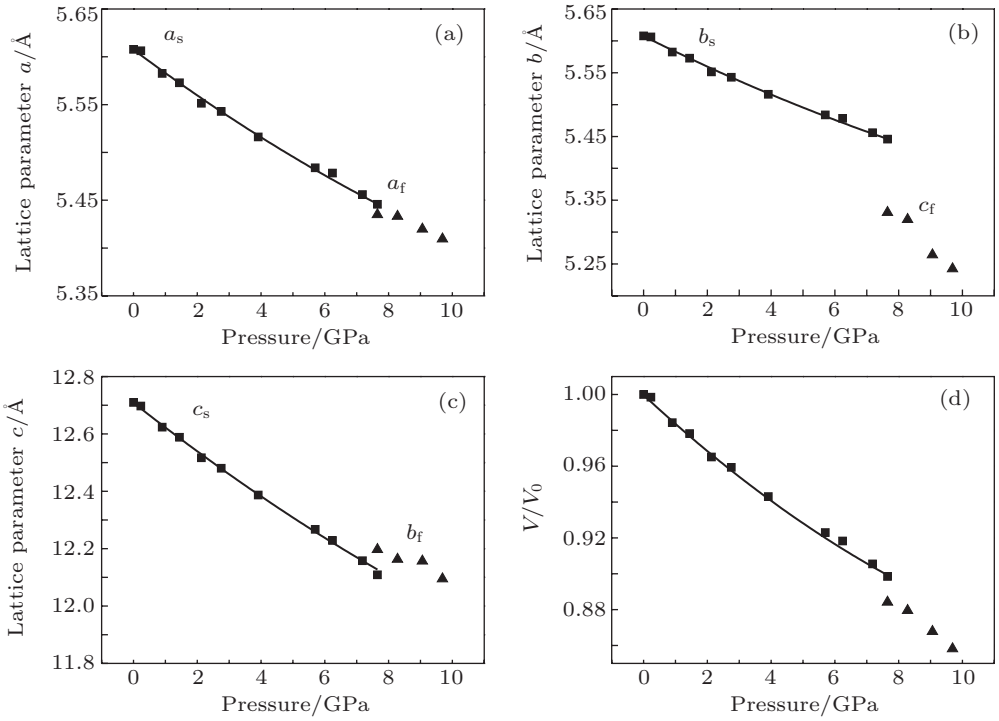

Fig. 6. (colour online) Evolutions of the lattice parameters and V/V_0 with pressure for the scheelite and the fergusonite phases of $BaWO_4$. Solid squares denote the data of the scheelite phase. Solid triangles refer to the fergusonite data. The subscripts s and f represent the scheelite and fergusonite phases respectively. In panels (a), (b), and (c) the solid lines are the quadratic fitting to the respective lattice parameters up to 7.7 GPa. In panel (d) the solid line refers to the fit of a third-order Birch–Murnaghan equation of state to the scheelite phase.

4. Conclusion

We carried out *in-situ* XRD and Raman experiments under hydrostatic pressure up to 9.7 GPa to investigate the nature of the scheelite-to-fergusonite transition in $BaWO_4$. The first-order characters are revealed unambiguously by a 1.6% volume collapse, coexistence of phases, and hysteresis on release of pressure. The analysis of atomic displacements shows that a coupling of large compression of soft BaO_8 polyhedrons to the small displacive distortion of rigid WO_4 tetrahedrons is responsible for the first-order ferroelastic transition. Such a coupling mechanism will have important material and mineralogical implications since many compounds and minerals crystallize into the scheelite structure and transform into the fergusonite structure under high pressure.

Acknowledgment

The authors would like to thank Liu Jing and her team of the Institute of High-Energy Physics, Chinese Academy of Sciences for their assistance with the high-pressure experiments and also the Photon Factory in Japan for providing synchrotron beamtime under Proposal No. 2009G124. This is project No. IS-1492 from the Guangzhou Institute of Geochemistry, Chinese Academy of Sciences.

References

[1] Dove M T 1997 *Am. Mineral* **82** 213

[2] Bragg W and Gibbs R E 1925 *Proceedings of the Royal Society of London Series a-Containing Papers of a Mathematical and Physical Character* **109** 405

[3] Dove M T, Gambhir M and Heine V 1999 *Phys. Chem. Miner.* **26** 344

[4] Fleury P A, Scott J F and Worlock J M 1968 *Phys. Rev. Lett.* **21** 16

[5] Hammonds K D, Dove M T, Giddy A P, Heine V and Winkler B 1996 *Am. Mineral* **81** 1057

[6] Giddy A P, Dove M T, Pawley G S and Heine V 1993 *Acta Crystallogr.* A **49** 697

[7] Sleight A 1972 *Acta Crystallogr.* B **28** 2899

[8] Nyman H, Hyde B G and Andersson S 1984 *Acta Crystallogr.* B **40** 441

[9] Panchal V, Garg N, Chauhan A K, Sangeeta B and Sharma S M 2004 *Solid State Commun.* **130** 203

[10] Errandonea D, Pellicer-Porres J, Manjon F J, Segura A, Ferrer-Roca C, Kumar R S, Tschauner O, Lopez-Solano J, Rodriguez-Hernandez P, Radescu S, Mujica A, Munoz A and Aquilanti G 2006 *Phys. Rev.* B **73** 224103

[11] Jayaraman A, Batlogg B and VanUitert L G 1983 *Phys. Rev.* B **28** 4774

[12] Manjon F J, Errandonea D, Garro N, Pellicer-Porres J, Rodriguez-Hernandez P, Radescu S, Lopez-Solano J, Mujica A and Munoz A 2006 *Phys. Rev.* B **74** 144111

[13] Errandonea D 2007 *Europhy. Lett.* **77** 56001

[14] Errandonea D and Manjon F J 2009 *Mater. Res. Bull.* **44** 807

[15] Lacomba-Perales R, Martínez-García D, Errandonea D, Le Godec Y, Philippe J and Morard G 2009 *High Press. Res.* **29** 76

[16] Klotz S, Chervin J C, Munsch P and Le Marchand G 2009 *J. Phys.* D: *Appl. Phys.* **42** 075413

[17] Angel R J, Bujak M, Zhao J, Gatta G D and Jacobsen S D 2007 *J. Appl. Crystallogr.* **40** 26

[18] Mao H K, Xu J and Bell P M 1986 *J. Geophys. Res.* **91** 4673

[19] Toby B H 2001 *J. Appl. Crystallogr.* **34** 210

[20] Stubican V S 1964 *J. Am. Ceram. Soc.* **47** 55

[21] David W I F 1983 *Mater. Res. Bull.* **18** 749

[22] Jian L and Wayman C M 1997 *J. Am. Ceram. Soc.* **80** 803

[23] Grzechnik A, Syassen K, Loa I, Hanfland M and Gesland J Y 2002 *Phys. Rev.* B **65** 104102

[24] Grzechnik A, Crichton W A, Hanfland M and van Smaalen S 2003 *J. Phys.: Condens. Matter* **15** 7261

[25] Errandonea D, Pellicer-Porres J, Manjon F J, Segura A, Ferrer-Roca C, Kumar R S, Tschauner O, Rodriguez-Hernandez P, Lopez-Solano J, Radescu S, Mujica A, Munoz A and Aquilanti G 2005 *Phys. Rev.* B **72** 174106

[26] Panchal V, Garg N and Sharma S M 2006 *J. Phys.: Condens. Matter* **18** 3917

[27] Errandonea D, Kumar R S, Ma X H and Tu C Y 2008 *J. Solid State Chem.* **181** 355

[28] Grzechnik A, Crichton W A, Marshall W G and Friese K 2006 *J. Phys.: Condens. Matter* **18** 3017

[29] Tan D Y, Xiao W S, Zhou W G, Song M S, Xiong X L and Chen M 2009 *Chin. Phys. Lett.* **26** 046301

[30] Hardcastle F D and Wachs I E 1995 *J. Raman Spectrosc.* **26** 397

[31] Ming L C, Shieh S R, Jayaraman A, Sharma S K and Kim Y H 1999 *J. Phys. Chem. Solids* **60** 69

[32] Jayaraman A, Shieh S R, Sharma S K, Ming L C and Wang S Y 2001 *J. Raman Spectrosc.* **32** 167